# Characterization of VO<sub>2</sub>-Based Reconfigurable Linear-to-Circular Polarization Converter

David West<sup>(1)</sup>, Mark Lust<sup>(2)</sup>, and Nima Ghalichechian<sup>(1)</sup>

(1) Georgia Institute of Technology, Atlanta, GA 30308, USA (dwest64@gatech.edu; nima.1@gatech.edu) (2) The Ohio State University, Columbus, OH 43212, USA (lust.50@buckeyemail.osu.edu)

Abstract—We present the quasi-optical free space measurement of a reconfigurable linear-to-circular polarization (LCP) converter. Reconfigurability is achieved using vanadium dioxide (VO<sub>2</sub>), a phase-change material (PCM) that experiences a reversible metal-insulator transition (MIT) at 68 °C. Preliminary measurement results for a static, non-reconfigurable device correlate well with simulations, validating the accuracy of the measurement setup. The static device achieved phase error below 20°, axial ratio below 3 dB, and insertion loss below 1 dB across the Ka uplink band (27.5–31 GHz). Measurement results for the full device with VO<sub>2</sub> switches will be presented at the conference.

#### I. Introduction

Interference is a significant challenge facing wireless communications systems, especially as wireless bands become more congested. Polarization diversity may be used to isolate concurrent electromagnetic (EM) waves and combat interference. Furthermore, circular polarization (CP) is more robust against multipath fading compared to linear polarization (LP), and CP is preferred in satcom for avoiding polarization mismatch [1]. As such, a reconfigurable aperture capable of generating right-hand or left-hand CP (RHCP or LHCP, respectively) in a single band is highly desirable for both satcom and terrestrial networks.

To achieve reconfigurability, we use vanadium dioxide (VO<sub>2</sub>), a phase change material (PCM) with a metal-insulator transition (MIT) at a relatively low temperature of 68 °C. Our group has previously explored using VO<sub>2</sub> for a mmWave antenna-coupled microbolometer with a high responsivity [2]. Building on this prior work, we designed a VO<sub>2</sub>-based, reconfigurable linear-to-circular polarization (LCP) converter operating in the Ka uplink band (27.5–31 GHz) [3].

The operating principle and unit cell of the LCP converter are shown in Fig. 1. Perpendicular sets of meanderlines are superimposed on the surface, with one set corresponding to RHCP and the other to LHCP.  $VO_2$  switches are used to activate and deactivate the meanderlines to select the output polarization. To thermally actuate the  $VO_2$ , dc bias is applied to the meanderlines, and integrated nickel-chromium (NiCr) resistors heat the  $VO_2$  above the transition temperature. The four LCP converter device layers are fabricated on silicon. Each layer is attached to a PCB using a pick-and-place process with silver epoxy as the bonding material. The PCBs are layered and joined together with soldered pins, providing mechanical stability and electrical ports for dc biasing ( $V_{in1}$ ,  $V_{in2}$ , and GND in Fig. 1).

In this work, we discuss the quasi-optical free-space measurement setup for characterizing the performance of the

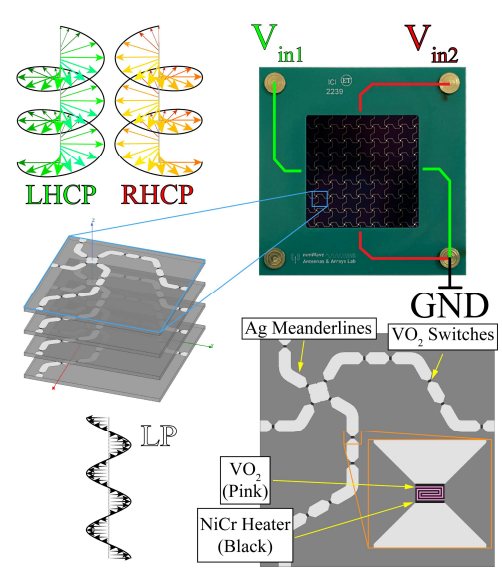


Fig. 1. Operating principle and unit cell design for the reconfigurable linear-to-circular polarization converter. Each set of meanderlines is individually biased to select right-hand or left-hand circular polarization.

VO<sub>2</sub>-based reconfigurable LCP converter. We present preliminary measurement results for a static, non-reconfigurable LCP converter, which validates the test setup and the operating principle of the device. Results for the fully reconfigurable device will be presented at the conference.

### II. MEASUREMENT SETUP

Quasi-optical free-space measurement setups have been used for measuring materials [4] as well as EM surfaces [1]. A diagram of the setup is shown in Fig. 2(a). We use a pair of Kaband spot-focusing lensed horn antennas. One antenna generates a Gaussian beam with a concentrated field intensity and a planar phase front at the focal plane, which is one focal length from the aperture (100 mm). The device under test (DUT) is centered on the focal point, where the electric field is at its maximum. A second lensed horn is placed two focal lengths away from the first antenna to receive the Gaussian beam. The setup emulates a plane wave incident on an infinite surface; thus, the results can be directly compared to Floquet port simulations.

A picture of the measurement setup is shown in Fig. 2(b). The horn antennas and the DUT are supported by 3D-printed fixtures. The horns are mounted on translating stages to allow adjustment along the axis of propagation, and the DUT is mounted on a rotating stage to permit measurements at oblique incidence. To prevent reflections from the optical table, the entire setup is elevated using 12 in. posts, and absorbers are

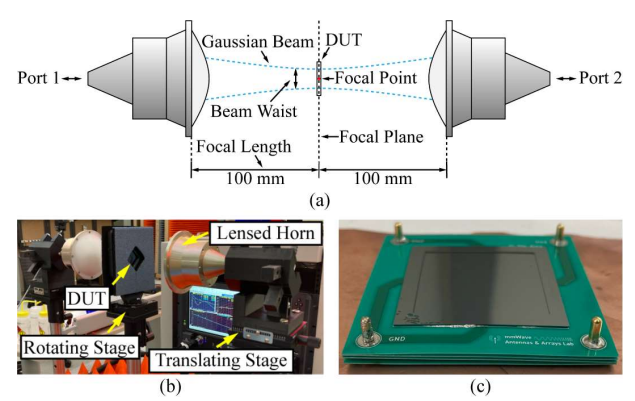


Fig. 2. (a) Schematic of the measurement setup. (b) Picture of the test setup. (c) Picture of the packaged four-layer LCP converter.

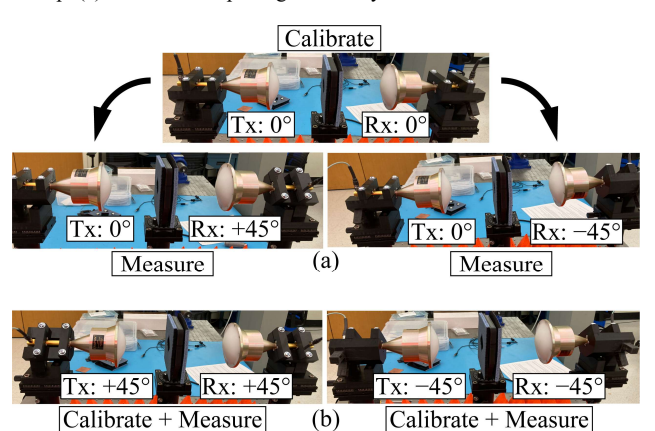


Fig. 3. Polarization configurations for the measurement setup. (a) Calibration with both antennas vertically polarized, followed by measurements with the receiving antenna tilted  $\pm 45^{\circ}$ . (b) Calibration and measurement with both antennas at  $\pm 45^{\circ}$ .

placed below. A picture of the packaged four-layer LCP converter is shown in Fig 2(c). A thru-reflect-line (TRL) calibration procedure is carried out as described in [4]. The DUT holder is included in the signal path during all calibration steps. To remove reflections from the receiving antenna and multipath effects, the time gating function of the VNA is employed.

The 3D-printed mounts are designed to allow a range of options for polarization of the antennas with respect to the metasurface, as shown in Fig. 3. The DUT is fixed at a 45° tilt in the holder. The antennas have a set of three pegs to allow independent tilt of the horns in 45° increments. To emulate the intended operation of the device, one antenna is placed upright using the center peg, as shown in Fig. 3(a). The incident LP wave is polarized at 45° relative to the meanderlines. The other antenna is tilted at ±45° using the left and right pegs, which captures the orthogonal components of the output CP wave. The components are expected to be 3 dB below the input signal and have a phase difference of 90°. In this case, calibration takes place with both antennas upright, and the  $S_{21}$  data is normalized to a measurement with an empty DUT holder and one tilted horn. Alternatively, both antennas can be tilted at  $\pm 45^{\circ}$  to capture the behavior of the orthogonal components individually, as shown in Fig. 3(b). In this case, separate calibrations are used for each of the components to minimize errors caused by repositioning the antennas.

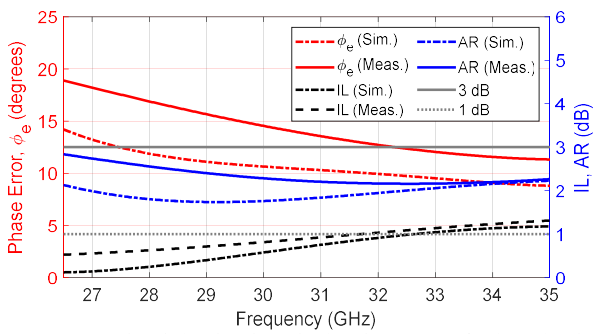


Fig. 4. Measured and simulated results for phase error  $(\phi_e)$ , insertion loss (IL), and axial ratio (AR) for the static LCP converter. The measured results correlate well with the simulation.

#### III. RESULTS AND CONCLUSION

Measurement results for a static, non-reconfigurable LCP converter are shown in Fig. 4 with comparisons to Ansys HFSS Floquet port simulation results. The  $S_{2l}$  data for the orthogonal field components were captured using the methodology shown in Fig. 3(b). The static device emulates having one set of meanderlines activated in the fully reconfigurable converter. The VO<sub>2</sub> switches are replaced with open connections for the inactive set of meanderlines and shorts for the active set.

The  $S_{21}$  data were used to calculate phase error  $(\phi_e)$  and axial ratio (AR) based on equations from [5], and the insertion loss (IL) was calculated as the average of the  $S_{21}$  magnitudes. Because the static device does not have VO<sub>2</sub> switches or heaters, the figures of merit are expected to deviate from the originally designed values. Additionally, the spacings between layers were greater than the designed value of 600 µm, with an average deviation of 230 µm. The spacing in the simulation has been adjusted to match the spacing of the assembled device. Methods for better controlling the layer spacing are being investigated for the final device. The performance of the static polarizer device is still acceptable, with  $\phi_e$  less than 20°, IL below 1 dB, and AR below 3 dB across the Ka uplink band. The results also correlate well with the simulation, validating the experimental setup. Measurement results for the fully reconfigurable device will be presented at the conference.

## REFERENCES

- [1] M. Del Mastro, M. Ettorre, and A. Grbic, "Dual-band, orthogonally-polarized LP-to-CP converter for satcom applications," *IEEE Trans. Antennas Propag.*, vol. 68, no. 9, pp. 6764-6776, 2020.
- [2] S. Chen, M. Lust, and N. Ghalichechian, "Antenna-coupled microbolometer based on VO<sub>2</sub>'s non-linear properties across the metal– insulator transition region," *Appl. Phys. Lett.*, vol. 121, no. 20, p. 201901, 2022.
- [3] M. Lust and N. Ghalichechian, "VO<sub>2</sub>-based reconfigurable meanderline polarizer at Ka-band," presented at the 2021 IEEE Int. Symp. Antennas Propag. & USNC-URSI Radio Sci. Meeting, 2021.
- [4] D. K. Ghodgaonkar, V. V. Varadan, and V. K. Varadan, "Free-space measurement of complex permittivity and complex permeability of magnetic materials at microwave frequencies," *IEEE Trans. Instrum. Meas.*, vol. 39, no. 2, pp. 387-394, 1990.
- [5] S. V. Parekh, "Simple formulae for circular-polarization axial-ratio calculations," *IEEE Antennas Propag. Mag.*, vol. 33, no. 1, pp. 30-32, Feb. 1991